

# Characterize the Distribution and Behavior Significance of the Global Signal Measured by Resting-State Functional Connectivity in the Elderly

G. chen<sup>1</sup>, C. xie<sup>1</sup>, G. chen<sup>1</sup>, B. D. Ward<sup>1</sup>, W. li<sup>1</sup>, P. Antuono<sup>2</sup>, and S-J. H<sup>3</sup>

<sup>1</sup>biophysics, Medical College of Wisconsin, milwaukee, wisconsin, United States, <sup>2</sup>Neurology, Medical College of Wisconsin, milwaukee, wisconsin, United States,

<sup>3</sup>Psychiatry and Behavioral Medicine, Medical College of Wisconsin, milwaukee, wisconsin, United States

## Introduction:

In resting-state fMRI studies, the global variations of the low-frequency BOLD signal are often considered nuisance effects and are commonly removed using a general linear model technique. However, this global signal regression method has been shown to introduce anticorrelated (negative) activation and reduce the sensitivity for detecting correlated (positive) activation in resting-state networks (Murphy 2009, Gavrilescu 2002, Weissenbacher 2009). The dependence of these resting-state correlations and anticorrelations on global signal removal has raised important questions regarding the nature of the global signal, the validity of global signal removal and the appropriate interpretation of observed brain networks (Fox and Raichel 2009). A recent primate study indicated that the often discarded global component of fMRI fluctuations measured during the resting state is tightly coupled with underlying neural activity (Leopold 2010). In the present study, we investigated several properties of the global signal in human subjects and found that it was significantly correlated with behavioral scores.

## Material and Method:

**Subjects and Imaging acquisition:** Fifteen amnestic mild cognitively impaired (aMCI) and 18 cognitively normal (CN) subjects were included in the study. The study was conducted with Medical College of Wisconsin Institutional Review Board approval. Written informed consent was obtained from each participant. Geriatric Depression Scale and Rey Auditory Verbal Learning Test (RAVLT) were administered before the scan. Imaging was performed using a whole-body 3T Signa GE scanner. Sagittal resting-state functional MRI (fMRI) datasets of the whole brain were obtained in six minutes with a single-shot gradient echo-planar imaging pulse sequence. The fMRI imaging parameters were: TE of 25 ms, TR of 2 s, flip angle of 90°, 36 slices were obtained without gap; slice thickness was 4 mm with a matrix size of 64×64 and field of view of 24×24 cm. High-resolution SPGR 3D axial images were acquired for anatomical reference. The parameters were: TE/TR/TI of 4/10/450 ms, flip angle of 12°, number of slices of 144, slice thickness of 1 mm, matrix size of 256×192.

**Global Signal Distribution:** A series of preprocessing steps common to most fMRI analyses was conducted, using the Analysis of Functional NeuroImages (AFNI) software. The preprocessing includes allowing for T1-equilibration effects; slice-acquisition-dependent time shifts correction; despiking; motion correction; detrending; white matter and CSF. Then, the global signal is extracted by averaging all preprocessed brain voxel time series. To characterize the global signal distribution pattern in the brain, Pearson product-moment correlation coefficient (CC) between the global signal and all brain voxel time series are calculated as one individual's global signal distribution pattern. One sample *t*-test is used to find the group global signal distribution pattern for the Control and MCI groups. A two-sample *t*-test is for the difference pattern between groups. Multivariate regression analysis is used to find the behavior significance of the global signal distribution with the depression score (GDS), memory score (RAVLT) and interaction (GDS\*RAVLT).

## Results and Discussion:

**Group pattern:** The global signal distribution is widespread in the resting brain. Figure A shows the global signal distribution pattern in the control group, while Figure B shows the similar pattern in MCI group ( $P<0.05$ , multiple comparison corrected). Figure C shows the different global signal distribution patterns between the Control and MCI groups (two-sample *t*-test,  $p<0.05$ , corrected). The different brain areas in the left fusiform, left middle temporal gyrus, left thalamus, left inferior parietal lobe, left precuneus and left superior parietal lobe are primarily overlapped with the default mode network. This suggests that the global signal distribution is changed for the most part in the default mode area between the control and MCI groups. There are many different in cerebellar areas, but they are not shown here.

**Behavior significance:** The global signal distribution patterns are correlated with behavior; they are significantly correlated with the depression score (GDS), memory score (RAVLT) and their interaction (GDS\*RAVLT). Figure D shows where the global signal is significantly correlated with the GDS score ( $p<0.05$ ). Those areas are the right temporal gyrus, left and right precentral gyrus, right insula, left and right postcentral gyrus. Voxelwise multivariate regression analysis identified the main effect of the RAVLT-DR scores, GDS scores and their interaction on the global signal distribution. The main effect of the GDS scores on the global signal distribution was in the regions that included the bilateral pre- and postcentral gyrus, right temporal gyrus and insula (Figure D); the main effects of the RAVLT-DR scores on the global signal distribution were in the regions of the bilateral pre- and postcentral gyrus, right temporal gyrus and insula (Figure E); The interactive effects of the RAVLT-DR and GDS scores on the global signal distribution were seen in the right middle temporal gyrus and superior temporal gyrus, left pre- and postcentral gyrus and left precuneus (Figure F). These findings identified the biological significance of global fMRI signals in human brain. Clearly, the so-called "global signal" has biological significance.

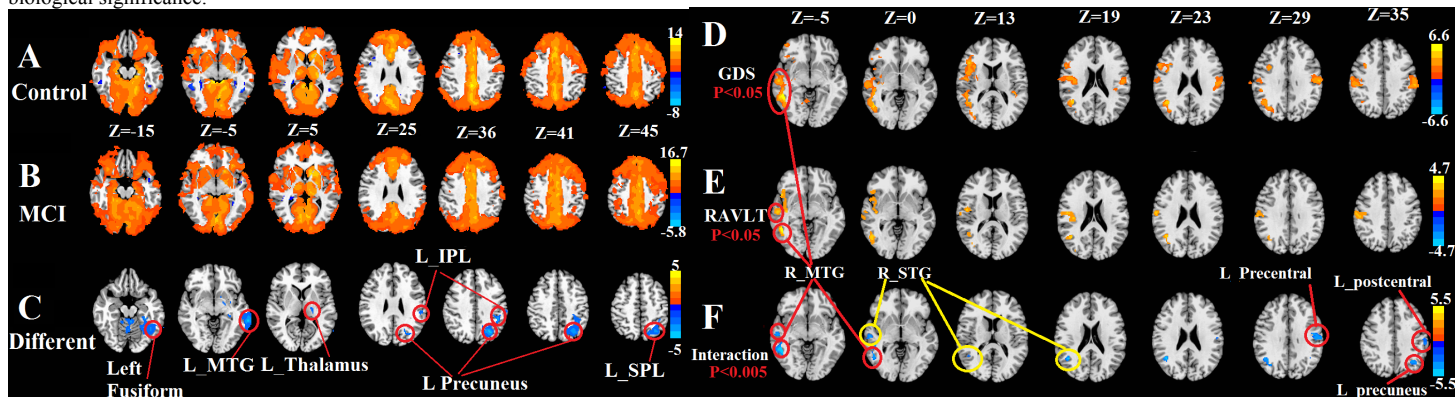


Figure A: global signal distribution pattern of Control group ( $P<0.05$ ). Figure B: global signal distribution pattern of MCI group ( $P<0.05$ ). Figure C: the different global signal distribution pattern between Control and MCI group using two-sample *t*-test ( $P<0.05$ ). Figure D: areas of global signal distribution pattern significantly correlated with GDS scores ( $P<0.05$ ). Figure E: areas of global signal distribution pattern significantly correlated with RAVLT scores ( $P<0.05$ ). Figure F: areas of global signal distribution pattern significantly correlated with the interaction (GDS\*RAVLT) of GDS and RAVLT scores ( $P<0.005$ ). All results are multiple comparison corrected.

**References:** 1. Scholvinck, M. L., A. Maier, et al. (2010). PNAS. 2. Scholvinck ML, et al. 2010 Jun 1;107(22):10238-43. 3. Murphy K, et al. Neuroimage. 2009 Feb 1;44(3):893-905. 4. Gavrilescu M, et al. Neuroimage. 2002 Oct;17(2):532-42. 5. Fox MD, et al. J Neurophysiol. 2009 Jun;101(6):3270-83. 6. Weissenbacher A, et al. Neuroimage. 2009 Oct 1;47(4):1408-16. 7. Chang C, Glover GH, et al. Neuroimage. 2009 Oct 1;47(4):1448-59. 8. Giove F, et al. Magn Reson Imaging. 2009 Oct;27(8):1058-64.

**ACKNOWLEDGEMENTS:** This work was supported by NIH-NIA R01 grant AD 20279 (SJJ) and NIH-NCRR CTSI grant 1-UL1-RR031973.